NIH Public Access
Author Manuscript
Free Radic Biol Med. Author manuscript; available in PMC 2015 July 01.

Published in final edited form as:
Free Radic Biol Med. 2014 July ; 72: 285–295. doi:10.1016/j.freeradbiomed.2014.04.022.

Catalytic Antioxidant Aeol 10150 Treatment Ameliorates Sulfur Mustard Analog 2-Chloroethyl Ethyl Sulfide Associated Cutaneous Toxic Effects

Neera Tewari-Singh[a], **Swetha Inturi**[a], **Anil K. Jain**[a], **Chapla Agarwal**[a], **David J Orlicky**[b], **Carl W. White**[c], **Rajesh Agarwal**[a,1], and **Brian J. Day**[d,1]

[a]Department of Pharmaceutical Sciences, University of Colorado Denver, Aurora, CO 80045, USA

[b]Department of Pathology, University of Colorado Denver, Aurora, CO 80045, USA

[c]Department of Pediatrics , University of Colorado Denver, Aurora, CO 80045, USA

[d]Department of Medicine, National Jewish Health, Denver, CO 80206, USA

Abstract

Our previous studies and other published reports with the chemical warfare agent sulfur mustard (SM) and its analog 2-chloroethyl ethyl sulfide (CEES) have indicated a role of oxidative stress in skin injuries caused by these vesicating agents. We examined the effects of the catalytic antioxidant AEOL 10150 in attenuation of CEES-induced toxicity in our established skin injury models (skin epidermal cells and SKH-1 hairless mice) to validate the role of oxidative stress in the pathophysiology of mustard vesicating agents. Treatment of mouse epidermal JB6 and human HaCaT cells with AEOL 10150 (50 μM) 1 h post CEES exposure resulted in significant ($p<0.05$) reversal of CEES-induced decreases in both cell viability and DNA synthesis. Similarly, AEOL 10150 treatment 1 h after CEES exposure attenuated CEES-induced DNA damage in these cells. Similar AEOL 10150 treatments also caused significant ($p<0.05$) reversal of CEES-induced decreases in cell viability in normal human epidermal keratinocytes. Cytoplasmic and mitochondrial reactive oxygen species measurements showed that AEOL 10150 treatment drastically ameliorated the CEES-induced oxidative stress in both JB6 and HaCaT cells. Based on

© 2014 Elsevier Inc. All rights reserved.

Corresponding authors: Brian J. Day, PhD, Department of Medicine, National Jewish Health, 1400 Jackson St, Denver, CO 80206, USA Phone: 303-398-1121, Fax 303-270-2263. dayb@njhealth.org; Rajesh Agarwal, PhD, Department of Pharmaceutical Sciences, University of Colorado Denver School of Pharmacy 12700 East 19th Avenue, Box C238 P-15 Research 2, Aurora, CO 80045, USA Phone: 303-724-4055, Fax: 303-724-7266. Rajesh.Agarwal@ucdenver.edu.
[1]Equal senior authorship

For reprint request: Dr. Brian J Day, Department of Medicine, National Jewish Health, 1400 Jackson St, Denver, CO 80206, USA Phone: 303-398-1121, Fax 303-270-2263. dayb@njhealth.org or Dr. Rajesh Agarwal, Department of Pharmaceutical Sciences, University of Colorado Denver School of Pharmacy 12700 East 19th Ave, Box C238 P-15 Research 2, Aurora, CO 80045, USA. Phone: 303-724-4055, Fax: 303-724-7266. Email: Rajesh.Agarwal@ucdenver.edu

Conflict of Interest Statement: Dr. Day is a consultant for and holds equity in Aeolus Pharmaceuticals which is developing metalloporphyrins as potential therapeutic agents. The other authors declare that they have no conflicts of interest.

Publisher's Disclaimer: This is a PDF file of an unedited manuscript that has been accepted for publication. As a service to our customers we are providing this early version of the manuscript. The manuscript will undergo copyediting, typesetting, and review of the resulting proof before it is published in its final citable form. Please note that during the production process errors may be discovered which could affect the content, and all legal disclaimers that apply to the journal pertain.

NIH-PA Author Manuscript
NIH-PA Author Manuscript
NIH-PA Author Manuscript

NIH-PA Author Manuscript

NIH-PA Author Manuscript

NIH-PA Author Manuscript

AEOL 10150 pharmacokinetic studies in SKH-1 mouse skin, mice were treated with topical formulation plus subcutaneous (injection; 5 mg/kg) AEOL 10150, 1 h after CEES (4 mg/mouse) exposure and every 4 h thereafter for 12 h. This AEOL 10150 treatment regimen resulted in over 50% ($p<0.05$) reversal in CEES-induced skin bi-fold and epidermal thickness, myeloperoxidase activity, and DNA oxidation in mouse skin. Results from this study demonstrate potential therapeutic efficacy of AEOL 10150 against CEES-mediated cutaneous lesions supporting AEOL 10150 as a medical countermeasure against SM-induced skin injuries.

Introduction

Since its first use in World War I by Germany, the vesicating agent sulfur mustard (2,2′-dichloroethyl sulfide; SM) has been used in a number of conflicts as a warfare agent [1-3]. This agent poses a potential warfare and terrorist threat for deliberate use and possible accidental exposure [2, 4]. Exposure to this vesicant is associated with early erythema and discomfort, which then leads to painful skin injuries including delayed blistering followed by ulceration, desquamation and necrosis [4-6]. These injuries occur largely due to the sensitivity of epidermal keartinocytes to SM where its DNA damaging ability is a major attribute [1, 7-9]. SM is a strong bifunctional alkylating agent forming adducts with cellular components of skin cells, mainly DNA, leading to DNA damage [3, 8-10]. In addition, its alkylating properties can also cause depletion of cellular thiols, mainly glutathione (GSH), and antioxidant enzymes in cells [11-13]. These events result in the accumulation of reactive oxygen species (ROS) causing lipid peroxidation, protein oxidation and DNA damage as critical components of SM-associated toxic cutaneous responses [3, 13, 14].

The monofunctional analog of SM, 2-chloroethyl ethyl sulfide (CEES), is extensively used to examine the toxic effects of SM including its DNA damaging properties [15-18]. Like SM, the DNA damage produced by CEES is also reported to be due to its direct alkylating effects, and increased ROS production, that leads to comparable toxic lesions from both these agents [10, 15]. Use of antioxidants or inhibitors of ROS formation in both SM and CEES animal models of skin injury have further indicated the role of oxidative stress in vesicant-induced skin injury [3, 12, 19, 20].

Use of antioxidants has shown some degree of protection against SM-induced cutaneous effects [20]. The catalytic metalloporphyrin, Mn(III) tetrakis(N,N′-diethylimidizolium-2-yl) porphyrin (AEOL 10150), is a small molecular weight antioxidant that possesses superoxide dismutase (SOD) and catalase like activities and inhibits lipid peroxidation [21-23]. Recent reports show that AEOL 10150 treatment 1 h after CEES exposure is effective in reducing CEES-induced lung cell toxicity by ameliorating mitochondrial dysfunction, ROS, DNA oxidation, and decrease in GSH in human bronchial epithelial cells (16HBE) and primary small airway epithelial (SAE) cells [24]. In vivo studies demonstrate that AEOL 10150 was an effective rescue agent against CEES-induced lung injury, inflammation and oxidative stress, and also improved CEES-induced olfactory epithelial injury [25, 26]. This antioxidant is reported as an effective treatment against Cl_2 lung injuries and radiation-induced pulmonary toxicity [23, 27].

NIH-PA Author Manuscript

NIH-PA Author Manuscript

NIH-PA Author Manuscript

The aim of this study was to examine the therapeutic potential of AEOL 10150 in ameliorating SM analog CEES-induced cutaneous effects when given 1 h after topical CEES exposure. Efficacy studies with this agent were carried out employing CEES-induced injury biomarkers, reported from our earlier studies, in skin epidermal (mouse JB6 and human HaCaT) cells and SKH-1 hairless mouse skin. The results from this study indicate the therapeutic potential of AEOL 10150 in reversing CEES-induced skin injury thus rationale for its further investigation as antioxidant therapy in vesicant-induced skin injury.

Materials and Methods

Cell culture and their treatment

JB6 and HaCaT cells (American Type Culture Collection; ATCC; Manassas, VA) were cultured as described earlier [19, 28]. Briefly, JB6 cells and HaCaT cells were cultured in MEM (with 5% heat inactivated FBS and 25 μg/ml gentamycin), and DMEM (with 10% FBS and 100 U/ml penicillin G-100 μg/ml streptomycin sulfate), respectively. Normal human epidermal keratinocytes (NHEK) were obtained from Lonza (Walkersville, MD), and cultured in the Keratinocyte Growth Medium (KGM) with provided additives. Cells grown O/N under standard culture conditions were treated with either DMSO (vehicle control) alone, CEES (0.25 or 0.5 mM) alone, AEOL 10150 (50 μM; Aeolus Pharmaceuticals, Mission Viejo, CA, USA) alone, or with AEOL 10150 (50 μM) 1 h after CEES (0.25 or 0.5 mM) topical exposure. A 50 μM concentration of AEOL 10150 given 1 h after CEES exposure was found to be effective in ameliorating CEES-induced cytotoxic effects in primary human primary small airway epithelial (SAE) cells [24]. Therefore, we tested the potential from 5 to100 μM AEOL 10150 concentrations in reversing CEES-induced cytotoxicity in JB6 and HaCaT cells (data not shown). Based on the results from these studies the 50 μM AEOL 10150 dose was determined to be optimal and this AEOL 10150 dose was used for further efficacy studies in these cells. CEES concentrations were obtained from stock prepared in DMSO. CEES was mixed into the cell growth media and added immediately to the 70-80% confluent cells as previously reported [28]. The final concentration of DMSO in the culture medium during treatments did not exceed 0.1% (v/v). All CEES preparations and treatments were employed using required and approved personal protective equipment under a safety laminar hood [16]

Measurement of cell viability and cell proliferation (DNA synthesis)

The cell viability (MTT) and cell proliferation (BrdU) assays were carried out as previously described [19, 28] 48 h following CEES exposure. For MTT assay, cells were incubated with 1 mg/ml of MTT (1 mg/mL of MTT; Sigma-Aldrich Chemical Co) in growth medium for 4 h at 37°C. The MTT solution then was removed, 100 μl DMSO added and absorbance was read at 540 nm. BrdU assay was carried out using BrdU colorimetric kit (Roche Applied Science, Indianapolis, IN). In brief, cells were fixed and DNA denatured after incubation with BrdU, and then labeled with anti-BrdU mouse monoclonal Ab-Fab, and cellular DNA was detected via measuring the absorbance at 370 nm (reference wavelength: 492 nm). Absorbance for both assays was examined using Spectra max 190 microplate reader (Molecular Devices, Sunnyvale, CA) and the blank control readings were subtracted from all the sample readings taken.

NIH-PA Author Manuscript

NIH-PA Author Manuscript

NIH-PA Author Manuscript

Comet Assay

Following the desired exposure and treatments, DNA damage was measured 2 h after CEES exposure via single cell gel electrophoresis (SCGE) or alkaline comet assay (pH ≥ 13) as described earlier [10]. In brief, the agarose precoated slides with cell suspension (300 μl) in 1 ml 1% low-melting point agarose were left at 4°C in the dark overnight in lysis solution. Thereafter, slides were washed, left for unwinding of DNA for 30 min and subjected to electrophoresis for 20 min at 22 V and 200 mA. The slides were then neutralized (500 mM Tris-HCl, pH 8.0), washed, and stained with 3 μg/ml of PI. The slides were dried overnight and scored for comets under Nikon invert microscope (Nikon Eclipse TE300) at x200 magnification. Images were captured using an attached CoolSNAP$_{ES}$ CCD camera. Tail extent moment (TEM; product of tail length and percentage tail DNA) of cells (50 each on triplicate slides) was scored using Komet 5.5 software (ANDOR Technology, South Windsor, CT).

Cellular and mitochondrial reactive oxygen species detection

Cellular and mitochondrial reactive oxygen species were measured in cells following the desired exposures and treatment for 4 or 6 h employing MitoSOX Red (Invitrogen; Carlsbad, CA) or dihydroethidium (DHE; 5 μM), respectively, as detailed earlier [10]. After 30 min or 1 h incubation with DHE or MitoSOX Red, respectively, cells were washed with 1X PBS, scraped and collected for live cell fluorescence determination via flowcytometry. Fluorescence was measured at the core services at the University of Colorado Cancer Center. Cells were treated with either 30 μM antimycin A for 20 min or 200 nM valinomycin for 1 h for the selectivity of MitoSOX red or DHE staining (positive controls), respectively.

Animal treatment

Male SKH-1 hairless mice (4 to 5 weeks old; Charles River Laboratories, Wilmington, MA) were housed at the Center of Laboratory Animal Care, University of Colorado Denver, CO. Mice were acclimatized and studies were carried out according to the specified protocol approved by the IACUC of the University of Colorado Denver as published earlier [19]. CEES (4 mg/mouse) was applied on to the dorsal skin of mice (approx. 8cm^2) in 200 μl acetone. AEOL 10150 was formulated into a topical gel formulation using a formulation previously described for highly positively charged agents and consisted of Tefose 63, Labrafil M 1944 and hydroxyethylcellulose [29]. AEOL 10150 topical gel formulation (700 μl/mouse of 1 mM concentration) was applied on to the dorsal skin exposed to CEES and AEOL 10150 given as subcutaneous injection (5mg/kg mouse) on the right thigh. The 4mg/mouse CEES dose was based on our earlier reported studies in SKH-1 mice where this CEES dose also caused microvesication, and biomarkers used in this study have been established using this dose of CEES (17, 29). The groups (n=5) shown in results are: a) CONTROL group shown here is vehicle (acetone) control but also represents i) untreated control and ii) acetone + AEOL 10150 (subcutaneous + topical gel formulation AEOL 10150) as no significant difference was found among these groups; b) CEES group shown here is topical CEES (4 mg) alone but also represents CEES + AEOL 10150 vehicles (subcutaneous vehicle (PBS) + topical gel formulation vehicle) as no significant difference

NIH-PA Author Manuscript

NIH-PA Author Manuscript

NIH-PA Author Manuscript

was found among these groups; c) CEES + AEOL 10150 (subcutaneous + topical gel formulation). All AEOL 10150 treatments were carried out 1 h after topical CEES exposure and every 4 h thereafter. This was based on pharmacokinetic studies in SKH-1 mouse skin after subcutaneous treatment and dose regiments shown effective in treating CEES-induced the lung injury [25]. In addition, subcutaneous+ topical treatment was also tested because combination of subcutaneous and intranasal delivery was effective in decreasing olfactory epithelial injury [26]. CEES topical dose of 4 mg was chosen as this dose showed maximum changes in the studied biomarkers reported earlier by us in this mouse strain [16, 30]. At 12 h of CEES exposure and treatments, skin bi-fold thickness was measured, mice were euthanized, dorsal skin was collected and either snap frozen in liquid nitrogen or fixed in formalin as detailed earlier [16].

Estimation of AEOL 10150 levels in skin tissue

This was carried out in the skin tissue collected from control (VC, acetone control; SC, subcutaneous AEOL 10150; TOF+SC, topical formulation +subcutaneous AEOL 10150; CEES, CEES exposure alone) and treatment [CEES+AEOL 10150 (SC or TOF +SC, subcutaneous or topical formulation + subcutaneous AEOL 10150 1 h after CEES exposure)] groups after 15 min, 1, 2, and 4 h of AEOL 10150 treatments (at same time from control groups) as previously described by [26]. Briefly, 30∼90 mg of skin tissues were homogenized (Ultra-Turrax T25) in 0.1N perchloric acid on ice, then the homogenate and plasma samples were deproteinated with perchloric acid, followed by centrifuge at 20,000g for 12 min. AEOL 10150 levels in the supernatants were measured using HPLC with spectrophotometric detection. A 20 uL sample was injected into a HPLC equipped with a UVVis detector (Elite LaChrom System L-2420, Hitachi) and the 10150 peak was measured at 446 nm with a retention time of 2.92 minutes. AEOL10150 concentrations were determined from standard curves that were linear over the concentrations reported using AEOL 10123 as an internal standard. Recovery of 10150 from skin tissue and plasma samples was determined to be greater than 98% and 99%, respectively.

Measurement of skin bi-fold thickness, epidermal thickness and quantification the number of incidences of microvesication

The dorsal skin bi-fold thickness was measured (mm) at 12 h in SKH-1 mice from control and treatment groups using an electronic digital caliper (Marathon Inc. Belleville, ON, Canada), by investigators blinded to treatment groups. Hematoxylin and eosin (H&E) staining of the mouse skin sections was carried as described earlier [16]. The epidermal thickness (μm) was measured in H&E stained skin tissue sections after 12 h of topical CEES exposure and treatments from all groups in at least 5 fields per tissue sample under a microscope using Axiovision Rel 4.5 software (×400 magnification; Carl Zeiss, Inc. Germany). The number of incidences of epidermal-dermal separation (microvesication) after 12 h of topical CEES exposure and treatments from all the groups was quantified from the H&E stained skin sections per skin section from all the sections examined per treatment group under a microscope using Axiovision Rel 4.5 software (×400 magnification; Carl Zeiss, Inc. Germany). The epidermal thickness measurements and counting of the incidences of microvesication were carried out after blinding the treatments or exposure on the slides, and these observations were further confirmed with the histopathologist.

NIH-PA Author Manuscript

NIH-PA Author Manuscript

NIH-PA Author Manuscript

Measurement of myeloperoxidase (MPO) activity

MPO activity was measured in the frozen skin tissue from the control and treatment groups employing a fluoro MPO kit from Cell Technology as published earlier [16]. In brief, ∼100 mg of skin tissue samples from each group were utilized to prepare lysates. Equal amounts of 50 μl reaction mixture and prepared sample (50 μg protein) or MPO standards were added in 96 well plates with reaction mixture as detailed in our earlier report [16]. After 1 h incubation in the dark at RT, fluorescence was measured at 530 nm excitation and 590 nm emission wavelengths using microplate fluorescence reader from Spectra Max Gemini EM (Sunnyvale, CA) . The blank control readings were subtracted from all the sample readings. The MPO activity was determined as mU/mL protein using the MPO standard curve.

Immunohistochemistry for 8-OHdG

Immunohistochemistry (IHC) of skin sections from all groups of mice in this study was carried out as reported earlier [16, 17]. Mouse skin sections (5 μm) were incubated with mouse monoclonal anti-8-oxo-2-deoxyguanosine (8-OHdG; JalCA, Japan) antibody in PBS O/N at 4°C in humidity chamber as reported earlier [17]. The N-Universal negative control rabbit IgG antibody (DAKO, Carpienteria, CA) was used as a negative control. Thereafter, after washing, sections were incubated with the appropriate biotinylated secondary antibody for 1 h, incubated with HRP-conjugated streptavidin (DAKO) for 30 min and DAB stained. Sections were counterstained with hematoxylin followed by dehydration steps, and mounted for microscopic observation [17]. The brown-colored DAB positive nuclei were counted from blinded slides of all the animal groups in 10 randomly selected fields (x400 magnification).

Statistical analyses

The data were analyzed using SigmaStat software version 2.03 (Jandel Scientific) for statistical significance of difference between CEES treated group versus control and other treatment groups. Significance was determined by one-way analysis of variance (oneway ANOVA) with Bonferroni or Tukey *t*-test for multiple comparisons. $P < 0.05$ was considered statistically significant

Results

AEOL 10150 treatment ameliorates CEES-induced decreases in cell viability, cell proliferation, and DNA damage in mouse and human skin epidermal cells

Our published studies have shown that CEES exposure caused a decrease in viability and proliferation of basal epidermal cells, which is mainly due to the DNA damaging effect of CEES observed in these cells [10, 28]. Hence, we first examined the effect of AEOL 10150 on CEES-induced cytotoxicity when given 1 h post CEES exposure in mouse and human epidermal cells. To assess cell viability, MTT assay of mouse epidermal JB6 cells and human epidermal HaCaT cells was performed following AEOL 10150 treatment (50 μM) 1 h after 0.25 mM CEES exposure for 48 h. The dose of 50 μM AEOL 10150 was selected following initial study where 1, 5, 10, 15, 25, 50 and 100 μM doses of AEOL 10150 were tested for reducing CEES-induced cell viability (data not shown). AEOL 10150 treatment

NIH-PA Author Manuscript

NIH-PA Author Manuscript

NIH-PA Author Manuscript

resulted in 70% and 34% ($p<0.05$) reversal in CEES-induced decrease in cell viability in JB6 and HaCaT cells, respectively (Fig.1A and B). Since AEOL 10150 50 μM treatment showed reversal in CEES-induced decrease in cell viability in JB6 and HaCaT cells, we further carried out MTT assay to confirm its efficacy in normal human epidermal keratinocytes (NHEK). Similar AEOL 10150 treatment caused a 39% ($p<0.05$) reversal in CEES-induced decrease in cell viability (Fig. 1C). AEOL 10150 treatment alone did not cause a significant ($p<0.05$) decrease in viability of mouse or human epidermal cells as compared to their respective controls (Fig. 1). However, since NHEK were difficult to grow, maintain and to carry out all studies, further studies were carried out in mouse JB6 and human HaCaT cells.

AEOL 10150 treatment demonstrated therapeutic efficacy in reversing CEES-induced decrease in cell viability in both mouse and human keratinocytes. We next examined AEOL 10150 effects on CEES-induced decreased cell proliferation using a BrdU assay (based on measurement of thymidine analog, BrdU incorporation during DNA synthesis) AEOL 10150 (50 μM) applied 1 h after 0.25 mM CEES exposure for 48 h in mouse JB6 and human HaCaT cells resulted in 43% ($p<0.05$) and 35% reversal, respectively, in CEES-induced decrease in cell proliferation in JB6 and HaCaT cells (Fig. 2A and B). AEOL 10150 treatment alone showed a 24% decrease in cell proliferation of JB6 cells as compared to control (Fig. 2).

The CEES-induced decrease in cell viability and proliferation could be associated with its DNA damaging effect as reported in our previous publication [10]. The comet assay is used to assess damaged DNA [10] and was employed to study the efficacy of AEOL 10150 in JB6 and HaCaT cells. Tail extent moment (TEM) was evaluated in these cells after 2 h of CEES exposure. AEOL 10150 treatment 1 h after CEES (0.5 mM) exposure caused a decrease in CEES-induced comet tail in both JB6 and HaCaT cells as seen in representative fluorescence micrographs (Fig. 2C and D top panel; red arrows). Quantification of TEM in these cells showed that AEOL 10150 treatment caused a 34% and 38% ($p<0.05$) reversal in CEES-induced DNA damage in JB6 and HaCaT cells, respectively (Fig. 2C and D). AEOL 10150 treatment alone did not cause significant ($p<0.05$) DNA damage as compared to controls in JB6 or HaCaT cells (Fig. 1).

AEOL 10150 treatment ameliorates CEES-induced oxidative stress in mouse and human skin epidermal cells

Following CEES exposure, an increase in oxidative stress and depletion of GSH have been related to its DNA damaging effect in our previous studies and reports by others [10, 12, 20, 24]. Since we observed that AEOL 10150 was effective in reversing CEES-induced DNA damage, we next assessed the efficacy of AEOL 10150 in reversing CEES-induced oxidative stress in JB6 and HaCaT cells. As reported earlier, we measured cellular and mitochondrial reactive oxygen species in skin epidermal cells employing DHE and MitoSOX red, respectively [10]. As seen in representative flow cytograms, CEES-induced cellular and mitochondrial reactive oxygen species were higher in HaCaT cells compared with JB6 cells (Figs. 3 and 4). Strong efficacy of AEOL 10150 was observed in reversing oxidative stress in both these cells (Figs. 3 and 4). As seen in representative flow cytograms

NIH-PA Author Manuscript

NIH-PA Author Manuscript

NIH-PA Author Manuscript

and quantified data, AEOL 10150 (50 μM) treatment 1 h after 0.5 mM CEES exposure for 6 h, resulted in complete reversal of CEES-induced cellular reactive oxygen species levels in both JB6 and HaCaT cells (Fig. 3A and B). In JB6 cells, 29% mitochondrial reactive oxygen species levels were observed after CEES exposure as compared to 5% in control cells. CEES exposed HaCaT cells evidenced 98% mitochondrial reactive oxygen species levels as compared to 3% in its respective control (Fig. 4). AEOL 10150 (50 μM) treatment applied 1 h after 0.5 mM CEES exposure for 4 h resulted in 97% and complete reversal of CEES-induced mitochondrial reactive oxygen species levels in both JB6 and HaCaT cells, respectively (Fig. 4A and B).

AEOL 10150 treatment ameliorates CEES-induced skin injuries and oxidative DNA damage in SKH-1 hairless mouse

Single dose therapy with subcutaneous AEOL 10150 was not effective against lung injuries due to CEES inhalation, and pharmacokinetic studies showed that by 8 h post injection plasma AEOL 10150 levels were near the level of detection [25]. To determine an effective dosing regimen for AEOL 10150 in skin tissue, we conducted pharmacokinetic investigations in skin samples from mice 0.25-4 h post AEOL 10150 treatment using HPLC analysis. Skin AEOL 10150 levels were higher after 15 min, 1 h and 2 h after AEOL 10150 combined (subcutaneous + topical) treatment as compared to its subcutaneous administration alone (Fig. 5). AEOL 10150 levels at 15 min, 1 h and 2 h following subcutaneous treatments after CEES exposures were 6.01, 2.02 and 1.01 pmol/mg skin tissue, respectively. Higher AEOL 10150 levels of 11.28, 3.50 and 1.97 pmol/mg skin tissue were recorded after its combined SC and topical administration for 15 min, 1 h and 2 h, respectively (Fig. 5). Similar AEOL 10150 levels (2.40 pmol/mg skin tissue) were observed 4 h after subcutaneous alone or its combined delivery (Fig.5). Based on these results and previous findings in lung tissue, AEOL 10150 combined treatment was given every 4 h after its initial administration through the study endpoint.

To examine the efficacy of combined AEOL 10150 route of administration, we analyzed the previously reported biomarkers of CEES-induced skin injury that includes skin bi-fold thickness, epidermal thickness, microvesication and MPO activity [16, 19, 30]. These skin injury indicators were analyzed in SKH-1 mice skin following either control or CEES exposure or AEOL 10150 combined treatment 1 h after CEES exposure, and every 4 h thereafter for 12 h. AEOL 10150 treatment resulted in 61% ($p<0.05$) and 53% ($p<0.05$) reversal of CEES-induced increases in skin bi-fold thickness (Fig. 6A) and epidermal thickness (Fig. 6B), respectively, in SKH-1 mice. Epidermal-dermal separation, which is an important consequence of vesicant skin injury, was quantified in H&E stained skin sections. As seen in representative pictures, AEOL 10150 combined treatment caused reversal in the size (green arrows) and numbers of CEES-induced epidermal-dermal separations (Fig. 7A). There was a trend for less CEES-induced microvesication (epidermal-dermal separations) events when dorsal skin of SKH-1 mice was treated with AEOL 10150 1 h after CEES exposure (Fig. 7A). However, reduction in this NM-induced lesion was not significant when NM+AEOL 10150 group was compared with NM alone exposure group. MPO activity, an indicator of neutrophil infiltration, is reported to increase after vesicating agent exposure in the skin tissue of mice. Similar treatment of CEES-exposed mouse skin with AEOL 10150

NIH-PA Author Manuscript

NIH-PA Author Manuscript

NIH-PA Author Manuscript

reported here resulted in 93% ($p<0.05$) reversal of CEES-induced increase in MPO activity (Fig. 7B).

Our previous findings indicate a role for oxidative stress in CEES-induced DNA damage leading to further toxic responses in epidermal cells and lesions in skin tissue of mice [10, 12, 19]. Hence, we examined the efficacy of antioxidant AEOL 10150 in reversing the CEES-induced oxidative DNA damage using IHC for 8-OHdG, an oxidized nucleoside of DNA. AEOL 10150 combined treatment caused a 67% decrease in the CEES-induced elevation of 8-OHdG positive cells as detected by brown stained nuclei in representative pictures (red arrows, Fig. 7C).

Discussion

There are currently no effective approved therapies against skin injuries caused by the vesicating agent SM. Though some benefit is obtained with decontamination and supportive treatment, if applied timely [1, 31]. Previous efforts to develop effective therapies to treat injuries from vesicant agents have reported that drugs targeting vesicant-induced oxidative stress may be helpful in attenuating vesicant-induced skin injuries [3, 12, 19, 20]. The current investigation indicates therapeutic efficacy of catalytic antioxidant AEOL 10150 in reversing CEES-induced toxic effects as well as oxidative DNA damage in skin epidermal cells and SKH-1 mouse skin. In addition to our previous reported studies, this study further highlights the role of oxidative stress in CEES-induced cutaneous damage and associated mechanisms reported in skin epidermal cells and mouse skin [12, 17-19].

With similar toxic effects to SM, CEES is a useful SM surrogate used to generate injury models and identify treatment agents [15, 24, 28]. However, it is a monofunctional alkylating agent and a less toxic analog of SM that forms adducts instead of cross-links with cellular molecules [10]. Therefore, the identified therapeutic efficacy of AEOL 10150 in this study needs to be further examined in the skin injury model with primary vesicating agents, SM and nitrogen mustard (NM). Basal epidermal skin keratinocytes are reported to be the primary targets of vesicating agents. Keratinocyte cell death also leads to protease digestion of anchoring filaments of the epidermal-dermal junction, thus forming blisters on skin tissue [5, 32]. Therefore, efficacy studies reported herein were carried out in mouse and human skin epidermal keratinocytes and SKH-1 hairless mouse skin using injury endpoints from our previously reported studies (Tewari-Singh et al., 2010; Inturi et al., 2011., Jain et al., 2011b).

Vesicating agents with strong alkylating properties can cause either direct DNA damage or interact with cellular thiols leads to the accumulation of ROS causing mainly lipid peroxidation, protein oxidation and DNA damage [10, 12, 20, 33]. CEES-induced DNA damage could lead to activation of DNA-damage related signaling pathways that cause cellular toxic responses including cell death as reported earlier [10, 17, 18, 28, 34]. In this study, 50 μM AEOL 10150 treatment applied 1 h after CEES exposure caused a reversal in CEES-induced loss of cell viability in mouse epidermal JB6 cells, human HaCaT, and NHEK (primary epidermal) cells. Similar AEOL 10150 treatment also caused a reversal in CEES-induced decrease in cell proliferation and increase in DNA damage in these cells. Our

NIH-PA Author Manuscript

NIH-PA Author Manuscript

NIH-PA Author Manuscript

results show that AEOL 10150 completely reversed CEES-induced cellular and mitochondrial ROS formation. These results indicate that AEOL 10150 can reverse CEES-induced oxidative stress and may lead to the observed effects on CEES-induced DNA damage and decreases in cell proliferation and cell viability in JB6 and HaCaT cells (Fig. 8). The results obtained in skin epidermal cells are comparable with similar dose and treatment regimen of AEOL 10150 which caused a reversal in CEES-induced cell viability, mitochondrial dysfunction, DNA oxidation, and ROS generation in human lung 16HBE and primary small airway epithelial cells [24]. Similar to the findings from this report in lung cells, mitochondrial oxidative stress was identified that could cause cellular oxidative stress and further toxic consequences. Although AEOL 10150 treatment caused complete reversal in cellular oxidative stress, its use as a treatment did not cause a complete reversal in CEES-induced DNA damage, DNA proliferation and cell viability. This could be due to direct DNA damage caused by the alkylating effects of CEES and the delayed application of the AEOL 10150 treatment (Fig. 8). Our earlier studies have shown that GSH treatment caused a reversal in CEES-induced depletion of GSH levels and CEES-induced cell toxicity [12]. Since AEOL 10150 treatment in lung cells caused a reversal in CEES-induced depletion of GSH levels [24], AEOL 10150 treatment could also have caused a reversal in CEES-induced decrease in GSH levels in skin epidermal cells related to oxidative stress. This study further suggests the role of GSH in CEES-caused skin injury; however, our previous study shows that GSH supplementation could protect the CEES-induced skin but its treatment efficacy was not strong when given after CEES exposure. Therefore, AEOL 10150 treatment could be a better option for reversing CEES-induced skin toxicity via increasing GSH levels, though further study is required in this direction.

Treatment with AEOL 10150 (5 mg/kg) 1 h after CEES exposure caused a significant reversal in CEES-induced lung injury [25]. In addition it's combined treatment (subcutaneous plus nasal delivery) 1 h after CEES exposure caused decreased olfactory epithelial injury rats [26]. With use based on these reports, pharmacokinetic study in SKH-1 mice skin showed higher of AEOL 10150 up to 2 h after its combined (subcutaneous, 5 mg/kg+topical) treatment as compared with only its subcutaneous treatment 1 h post-CEES exposure. Since AEOL 10150 levels in the skin following its combined treatment substantially decreased after 4 h of treatment, AEOL 10150 treatment 1 h after of CEES exposure was repeated every 4 h thereafter for 12 h total. Our earlier studies have shown that CEES-induced oxidative stress leading to oxidative DNA damage could play a key role in CEES-related inflammatory response and dermal injury in SKH-1 mice [17, 18]. Consistent with these reports, present studies show that treatment with the antioxidant AEOL 10150 caused a reversal in CEES-induced skin bi-fold thickness and MPO activity (indicating neutrophil infiltration and an inflammatory response) and oxidative DNA damage (Fig. 8). Since the infiltration of neutrophils could cause a further increase in ROS generation in the tissue leading to increased oxidative stress and more damage including lipid peroxidation, AEOL 10150 effect on reversal of CEES-induced MPO activity may be driving some of the observed reduction in CEES-induced skin injury. Increase in the vesicant-induced ROS generation following increase in inflammatory cells could be triggered via host defense mechanisms including inflammatory cytokines and chemokines, which are reported to increase following vesicant exposure and could be a potential target for catalytic antioxidant

NIH-PA Author Manuscript

NIH-PA Author Manuscript

NIH-PA Author Manuscript

therapy. Similar to this study, our earlier reported study where GSH was given 1 h before CEES exposure also protected mice against CEES-induced increase in skin bi-fold and epidermal thickness, apoptotic cell death, and MPO activity (12). This again suggests that AEOL 10150 treatment could also have caused a reversal in CEES-induced decrease in GSH levels in mouse skin. This study is in agreement with previous report where AEOL 10150 treatment reversed lung injury, inflammation and oxidative stress, indicating its effect in reversing skin and lung injuries with CEES [25].

AEOL 10150 is an antioxidant metalloporphyrin that scavenges hydrogen peroxide, superoxide, peroxynitrite and lipid peroxides [21, 35-37]. Our earlier studies have reported a CEES-induced O_2^- increase and lipid peroxidation, which could be due to depletion of antioxidant thiols like GSH, both of which could contribute to the reported CEES-induced oxidative DNA damage [10, 17, 18]. In addition, vesicating agents could react with cellular reductases causing changes in electron transfer and increased free radical production [38]. AEOL 10150 could directly scavenge oxidants or increase GSH levels to ameliorate the oxidative stress-related DNA damage and lipid peroxidation, which could be the reason for the reduction in CEES-induced increase in cytotoxicity, skin inflammation and microvesication seen in this study (Fig. 8). However, ROS may not be the only cause of CEES-induced skin inflammation and vesication [10, 17], which is also indicated by this study as AEOL 10150 almost completely suppressed CEES-induced cellular and mitochondrial ROS; however, did not comparatively reverse DNA damage and cell death. Therefore, apart from scavenging ROS there could be other mechanisms involved by which AEOL 10150 could ameliorate these toxic effects. Hence, further studies are needed to further explore the mechanisms of action of AEOL 10150 in reversing vesicant-induced skin injuries. Metalloporphyrins have been shown to have multiple mechanisms of action in complex biological systems. The decreased formation of ROS and protection of cellular macromolecules can occur through both direct and indirect actions of the metalloporphyrin on ROS formation and scavenging which have been recently reviewed [39]. Further determination of the pathways, especially related to oxidative stress, that are involved in the AEOL 10150-related efficacy in ameliorating vesicating agents-induced skin injuries will be of importance for optimizing its treatment alone or in combination with other agents.

Conclusions

Overall, the results here demonstrate the therapeutic potential of catalytic antioxidant AEOL 10150 in the rescue of CEES-induced cytotoxicity, skin injury, inflammation, and oxidative stress. This study further supports the testing and optimization of AEOL 10150 in skin injury models with the primary vesicating agents NM and SM.

Acknowledgments

This work was supported by the Countermeasures against Chemical Threats (CounterACT Program), National Institutes of Health Office of the Director, and the National Institute of Environmental Health Sciences, [Grant U54 ES-015678]. The study sponsors have no involvement in the study design; collection, analysis and interpretation of data; the writing of the manuscript; and the decision to submit the manuscript for publication.

NIH-PA Author Manuscript

NIH-PA Author Manuscript

NIH-PA Author Manuscript

References

1. Graham JS, Chilcott RP, Rice P, Milner SM, Hurst CG, Maliner BI. Wound healing of cutaneous sulfur mustard injuries: strategies for the development of improved therapies. J Burns Wounds. 2005; 4:e1. [PubMed: 16921406]
2. Graham JS, Schoneboom BA. Historical perspective on effects and treatment of sulfur mustard injuries. Chemico-biological interactions. 2013
3. Paromov V, Suntres Z, Smith M, Stone WL. Sulfur mustard toxicity following dermal exposure: role of oxidative stress, and antioxidant therapy. J Burns Wounds. 2007; 7:e7. [PubMed: 18091984]
4. Balali-Mood M, Hefazi M. The pharmacology, toxicology, and medical treatment of sulphur mustard poisoning. Fundam Clin Pharmacol. 2005; 19:297–315. [PubMed: 15910653]
5. Shakarjian MP, Heck DE, Gray JP, Sinko PJ, Gordon MK, Casillas RP, Heindel ND, Gerecke DR, Laskin DL, Laskin JD. Mechanisms mediating the vesicant actions of sulfur mustard after cutaneous exposure. Toxicol Sci. 2010; 114:5–19. [PubMed: 19833738]
6. Smith KJ, Smith WJ, Hamilton T, Skelton HG, Graham JS, Okerberg C, Moeller R, Hackley BE Jr. Histopathologic and immunohistochemical features in human skin after exposure to nitrogen and sulfur mustard. Am J Dermatopathol. 1998; 20:22–28. [PubMed: 9504665]
7. Dacre JC, Goldman M. Toxicology and pharmacology of the chemical warfare agent sulfur mustard. Pharmacol Rev. 1996; 48:289–326. [PubMed: 8804107]
8. Kehe K, Szinicz L. Medical aspects of sulphur mustard poisoning. Toxicology. 2005; 214:198–209. [PubMed: 16084004]
9. Papirmeister B, Gross CL, Meier HL, Petrali JP, Johnson JB. Molecular basis for mustard-induced vesication. Fundam Appl Toxicol. 1985; 5:S134–149. [PubMed: 2419197]
10. Inturi S, Tewari-Singh N, Gu M, Shrotriya S, Gomez J, Agarwal C, White CW, Agarwal R. Mechanisms of sulfur mustard analog 2-chloroethyl ethyl sulfide-induced DNA damage in skin epidermal cells and fibroblasts. Free radical biology & medicine. 2011; 51:2272–2280. [PubMed: 21920433]
11. Ghabili K, Agutter PS, Ghanei M, Ansarin K, Panahi Y, Shoja MM. Sulfur mustard toxicity: history, chemistry, pharmacokinetics, and pharmacodynamics. Critical reviews in toxicology. 2011; 41:384–403. [PubMed: 21329486]
12. Tewari-Singh N, Agarwal C, Huang J, Day BJ, White CW, Agarwal R. Efficacy of glutathione in ameliorating sulfur mustard analog-induced toxicity in cultured skin epidermal cells and in SKH-1 mouse skin in vivo. The Journal of pharmacology and experimental therapeutics. 2011; 336:450–459. [PubMed: 20974699]
13. Kehe K, Balszuweit F, Steinritz D, Thiermann H. Molecular toxicology of sulfur mustard-induced cutaneous inflammation and blistering. Toxicology. 2009; 263:12–19. [PubMed: 19651324]
14. Ruff AL, Dillman JF. Signaling molecules in sulfur mustard-induced cutaneous injury. Eplasty. 2007; 8:e2. [PubMed: 18213398]
15. Han S, Espinoza LA, Liao H, Boulares AH, Smulson ME. Protection by antioxidants against toxicity and apoptosis induced by the sulphur mustard analog 2-chloroethylethyl sulphide (CEES) in Jurkat T cells and normal human lymphocytes. Br J Pharmacol. 2004; 141:795–802. [PubMed: 14769780]
16. Tewari-Singh N, Rana S, Gu M, Pal A, Orlicky DJ, White CW, Agarwal R. Inflammatory biomarkers of sulfur mustard analog 2-chloroethyl ethyl sulfide-induced skin injury in SKH-1 hairless mice. Toxicol Sci. 2009; 108:194–206. [PubMed: 19075041]
17. Jain AK, Tewari-Singh N, Gu M, Inturi S, White CW, Agarwal R. Sulfur mustard analog, 2-chloroethyl ethyl sulfide-induced skin injury involves DNA damage and induction of inflammatory mediators, in part via oxidative stress, in SKH-1 hairless mouse skin. Toxicology letters. 2011; 205:293–301. [PubMed: 21722719]
18. Pal A, Tewari-Singh N, Gu M, Agarwal C, Huang J, Day BJ, White CW, Agarwal R. Sulfur mustard analog induces oxidative stress and activates signaling cascades in the skin of SKH-1 hairless mice. Free radical biology & medicine. 2009; 47:1640–1651. [PubMed: 19761830]

NIH-PA Author Manuscript

NIH-PA Author Manuscript

NIH-PA Author Manuscript

19. Tewari-Singh N, Jain AK, Inturi S, Agarwal C, White CW, Agarwal R. Silibinin attenuates sulfur mustard analog-induced skin injury by targeting multiple pathways connecting oxidative stress and inflammation. PloS one. 2012; 7:e46149. [PubMed: 23029417]
20. Laskin JD, Black AT, Jan YH, Sinko PJ, Heindel ND, Sunil V, Heck DE, Laskin DL. Oxidants and antioxidants in sulfur mustard-induced injury. Ann N Y Acad Sci. 2010; 1203:92–100. [PubMed: 20716289]
21. Kachadourian R, Johnson CA, Min E, Spasojevic I, Day BJ. Flavin-dependent antioxidant properties of a new series of meso-N,N′-dialkyl-imidazolium substituted manganese(III) porphyrins. Biochemical pharmacology. 2004; 67:77–85. [PubMed: 14667930]
22. Day BJ. Catalytic antioxidants: a radical approach to new therapeutics. Drug discovery today. 2004; 9:557–566. [PubMed: 15203091]
23. McGovern T, Day BJ, White CW, Powell WS, Martin JG. AEOL10150: a novel therapeutic for rescue treatment after toxic gas lung injury. Free radical biology & medicine. 2011; 50:602–608. [PubMed: 21156205]
24. Gould NS, White CW, Day BJ. A role for mitochondrial oxidative stress in sulfur mustard analog 2-chloroethyl ethyl sulfide-induced lung cell injury and antioxidant protection. The Journal of pharmacology and experimental therapeutics. 2009; 328:732–739. [PubMed: 19064720]
25. O'Neill HC, White CW, Veress LA, Hendry-Hofer TB, Loader JE, Min E, Huang J, Rancourt RC, Day BJ. Treatment with the catalytic metalloporphyrin AEOL 10150 reduces inflammation and oxidative stress due to inhalation of the sulfur mustard analog 2-chloroethyl ethyl sulfide. Free radical biology & medicine. 2010; 48:1188–1196. [PubMed: 20138141]
26. O'Neill HC, Orlicky DJ, Hendry-Hofer TB, Loader JE, Day BJ, White CW. Role of reactive oxygen and nitrogen species in olfactory epithelial injury by the sulfur mustard analogue 2-chloroethyl ethyl sulfide. American journal of respiratory cell and molecular biology. 2011; 45:323–331. [PubMed: 21642592]
27. Zhang Y, Zhang X, Rabbani ZN, Jackson IL, Vujaskovic Z. Oxidative stress mediates radiation lung injury by inducing apoptosis. International journal of radiation oncology, biology, physics. 2012; 83:740–748.
28. Tewari-Singh N, Gu M, Agarwal C, White CW, Agarwal R. Biological and molecular mechanisms of sulfur mustard analogue-induced toxicity in JB6 and HaCaT cells: possible role of ataxia telangiectasia-mutated/ataxia telangiectasia-Rad3-related cell cycle checkpoint pathway. Chem Res Toxicol. 2010; 23:1034–1044. [PubMed: 20469912]
29. Niazi, S. Handbook of Pharmaceutical Manufacturing Formulations, Semisolid Products. Boca Raton: CRC Press; 2004.
30. Jain AK, Tewari-Singh N, Orlicky DJ, White CW, Agarwal R. 2-Chloroethyl ethyl sulfide causes microvesication and inflammation-related histopathological changes in male hairless mouse skin. Toxicology. 2011; 282:129–138. [PubMed: 21295104]
31. Graham JS, Stevenson RS, Mitcheltree LW, Hamilton TA, Deckert RR, Lee RB, Schiavetta AM. Medical management of cutaneous sulfur mustard injuries. Toxicology. 2009; 263:47–58. [PubMed: 18762227]
32. Hayden PJ, Petrali JP, Stolper G, Hamilton TA, Jackson GR, Wertz PW, Ito S, Smith WJ, Klausner M. Microvesicating Effects of Sulfur Mustard on an In Vitro Human Skin Model. Toxicol In Vitro. 2009
33. Naghii MR. Sulfur mustard intoxication, oxidative stress, and antioxidants. Mil Med. 2002; 167:573–575. [PubMed: 12125850]
34. Black AT, Joseph LB, Casillas RP, Heck DE, Gerecke DR, Sinko PJ, Laskin DL, Laskin JD. Role of MAP kinases in regulating expression of antioxidants and inflammatory mediators in mouse keratinocytes following exposure to the half mustard, 2-chloroethyl ethyl sulfide. Toxicol Appl Pharmacol. 2010; 245:352–360. [PubMed: 20382172]
35. Day BJ, Fridovich I, Crapo JD. Manganic porphyrins possess catalase activity and protect endothelial cells against hydrogen peroxide-mediated injury. Archives of biochemistry and biophysics. 1997; 347:256–262. [PubMed: 9367533]
36. Day BJ, Batinic-Haberle I, Crapo JD. Metalloporphyrins are potent inhibitors of lipid peroxidation. Free radical biology & medicine. 1999; 26:730–736. [PubMed: 10218663]

NIH-PA Author Manuscript

NIH-PA Author Manuscript

NIH-PA Author Manuscript

37. Pfeiffer S, Schrammel A, Koesling D, Schmidt K, Mayer B. Molecular actions of a Mn(III)Porphyrin superoxide dismutase mimetic and peroxynitrite scavenger: reaction with nitric oxide and direct inhibition of NO synthase and soluble guanylyl cyclase. Molecular pharmacology. 1998; 53:795–800. [PubMed: 9547373]

38. Brimfield AA, Mancebo AM, Mason RP, Jiang JJ, Siraki AG, Novak MJ. Free radical production from the interaction of 2-chloroethyl vesicants (mustard gas) with pyridine nucleotide-driven flavoprotein electron transport systems. Toxicol Appl Pharmacol. 2009; 234:128–134. [PubMed: 18977373]

39. Day BJ. Antioxidant therapeutics: Pandora's box. Free radical biology & medicine. 2014; 66:58–64. [PubMed: 23856377]

Abbreviations

AEOL 10150	Mn (III) tetrakis (N,N′-diethylimidizolium-2-yl)portphyrin
BrdU	5-bromo-2′-deoxy-uridine
CEES	2-chloroethyl ethyl sulfide
DHE	dihydroethidium
GSH	reduced glutathione
16HBE cells	human bronchial epithelial cells
SAE cells	primary small airway epithelial cells
NHEK	Normal human epidermal keratinocytes
IHC	Immunohistochemistry
MPO	myeloperoxidase
8-OHdG	anti-8-oxo-2-deoxyguanosine
ROS	reactive oxygen species
SOD	superoxide dismutase
SC	subcutaneous
SCGE	single cell gel electrophoresis
TOF+SC	topical formulation +subcutaneous

NIH-PA Author Manuscript

NIH-PA Author Manuscript

NIH-PA Author Manuscript

Highlights

- The sulfur mustard analog CEES is a skin vesicant that produces oxidative stress.
- AEOL 10150 suppressed CEES-induced ROS and DNA damage in vitro and DNA oxidation in vivo.
- AEOL 10150 attenuated CEES-induced dermal injury both in vitro and in vivo.
- AEOL 10150 may be an effective medical countermeasure against CEES-induced skin injury.

NIH-PA Author Manuscript

NIH-PA Author Manuscript

NIH-PA Author Manuscript

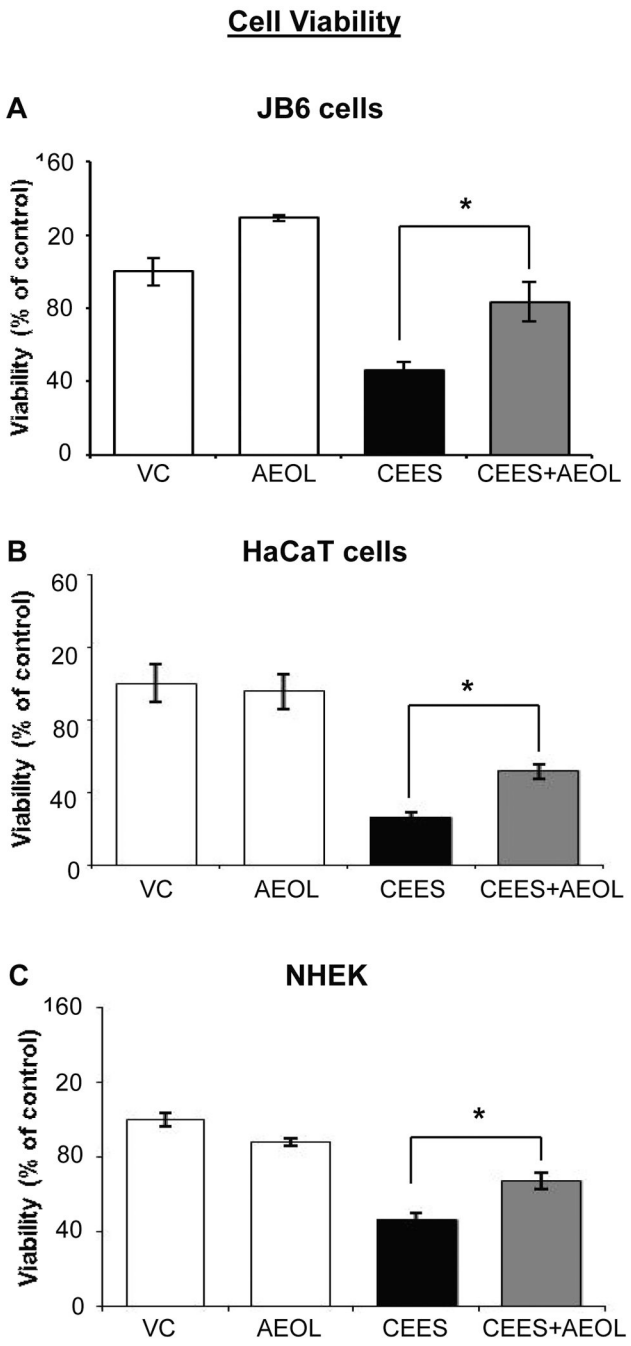

Figure 1. AEOL 10150 treatment ameliorates CEES-induced decreases in cell viability in mouse skin epidermal JB6 cells, human skin epidermal HaCaT cells, and NHEK

Mouse epidermal JB6 (A), human epidermal HaCaT cells (B), and NHEK (C) were seeded and grown overnight in 96 well plates. These cells were then exposed to either DMSO alone (VC), 50 μM AEOL 10150 alone (AEOL), 0.25 mM CEES in DMSO (CEES), or to 50 μM AEOL 10150 1 h after 0.25 mM CEES exposure (CEES+AEOL) for 48 h. Thereafter, MTT assay was carried out as described under Materials and Methods. Data shown are mean ± SEM of 4-6 independent samples for each treatment. *, $p<0.05$ as compared to CEES exposed group.

NIH-PA Author Manuscript
NIH-PA Author Manuscript
NIH-PA Author Manuscript

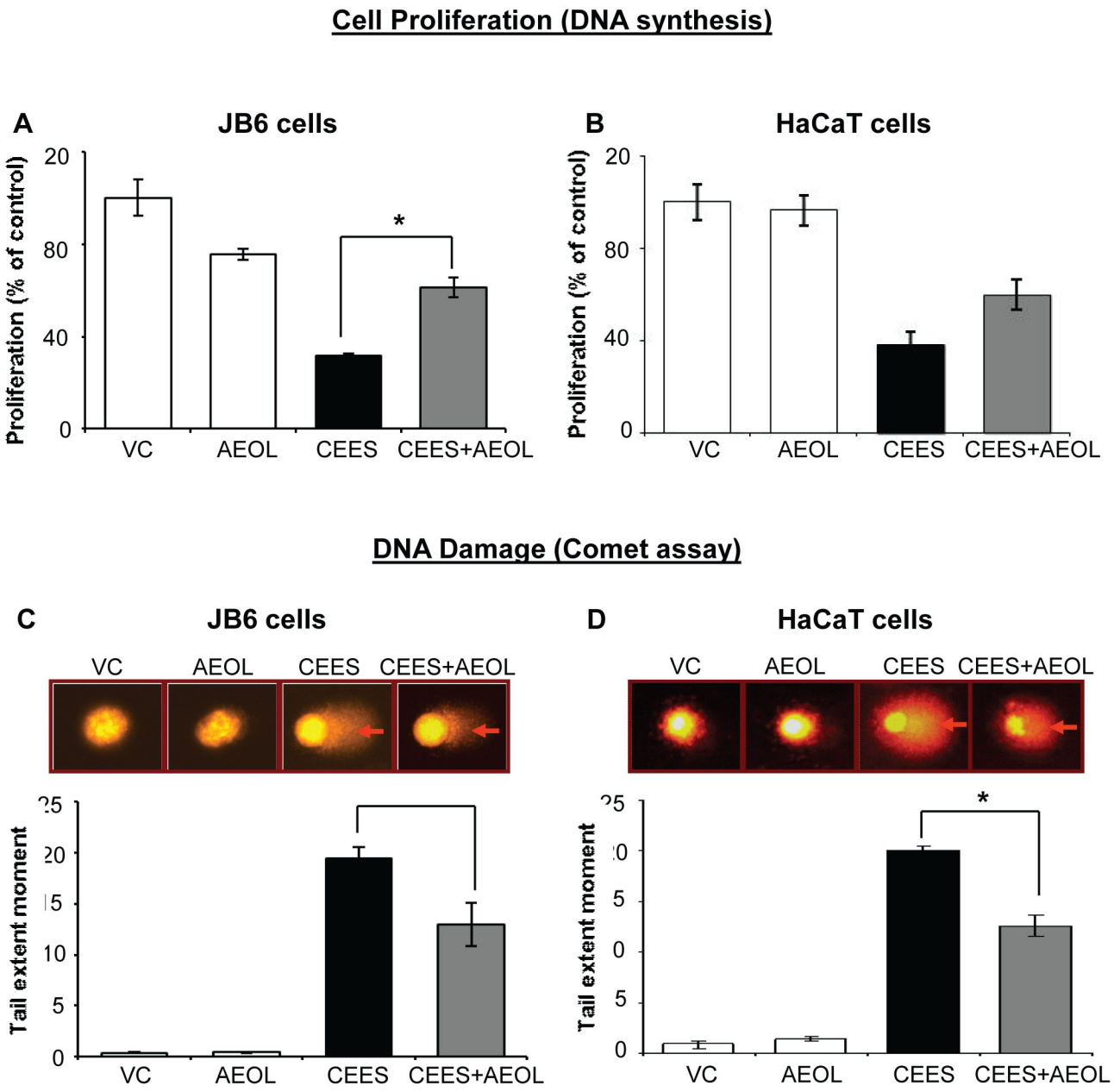

Figure 2. AEOL 10150 treatment ameliorates CEES-induced decrease in DNA synthesis and DNA damage in mouse skin epidermal JB6 cells and human skin epidermal HaCaT cells

Mouse epidermal JB6 (A) and human epidermal HaCaT cells (B) were seeded and grown overnight in 96 well plates. These cells were then exposed to either DMSO alone (VC), 50 μM AEOL 10150 alone (AEOL), 0.25 mM CEES in DMSO (CEES), or to 50 μM AEOL 10150 1 h after 0.25 mM CEES exposure (CEES+AEOL) for 48 h. Thereafter, cells were incubated with BrdU for 2 h, fixed and DNA denatured and labeled with anti-BrdU mouse monoclonal Ab-Fab, and product was quantified by measuring the absorbance as detailed under Materials and Methods (A and B). After desired exposure and treatments as above for 2 h, DNA damage in the cells was measured via alkaline comet assay as detailed under Materials and Methods (C and D). Representative pictures show damaged DNA seen in the

form of comets behind the JB6 (C) and HaCaT (D) cells, which was scored as the tail extent moment (TEM; product of tail length and percentage tail DNA). Data shown are mean ± SEM of 3-4 independent samples. *, $p<0.05$ as compared to CEES exposed group.

NIH-PA Author Manuscript
NIH-PA Author Manuscript
NIH-PA Author Manuscript

NIH-PA Author Manuscript
NIH-PA Author Manuscript
NIH-PA Author Manuscript

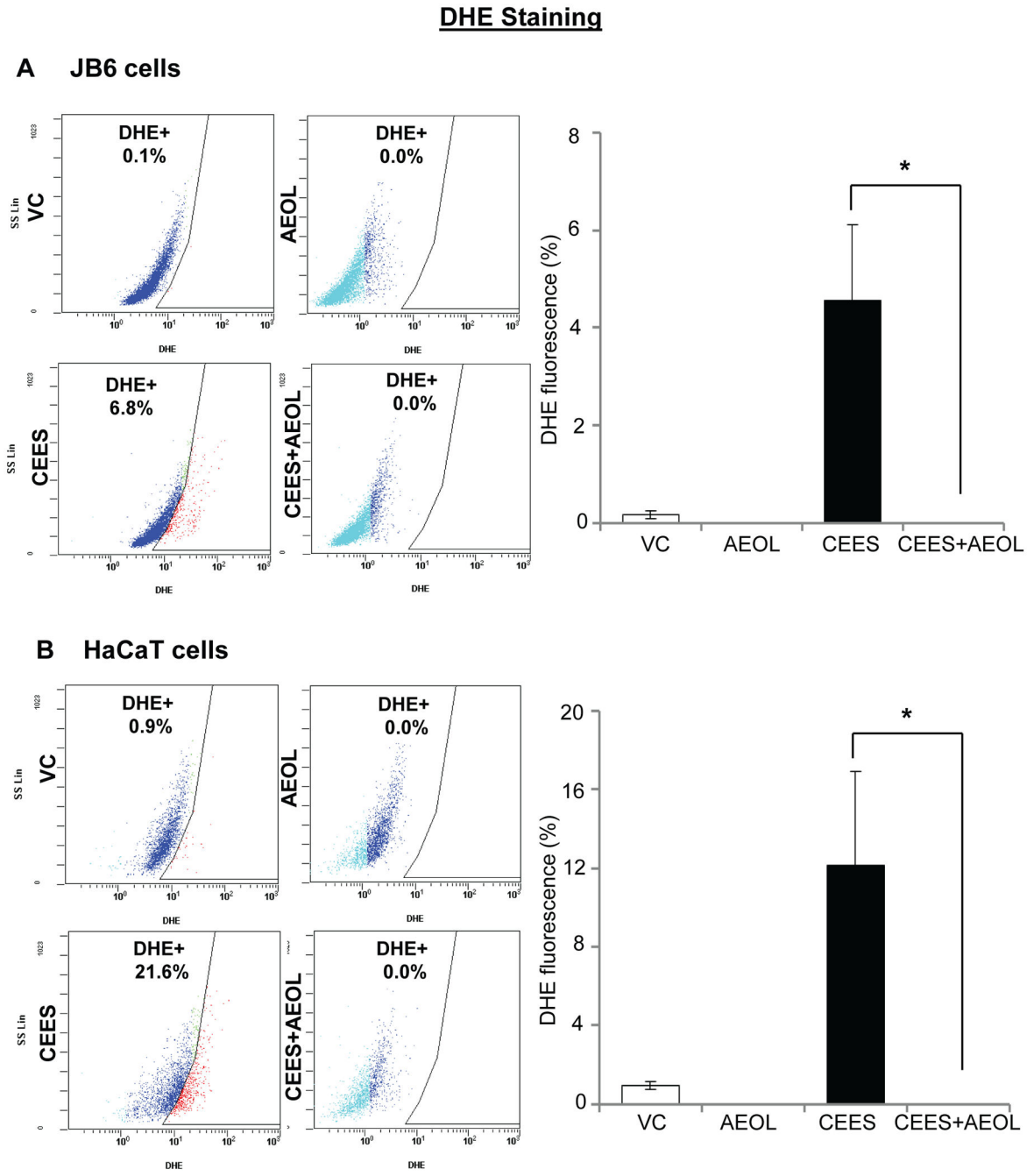

Figure 3. AEOL 10150 treatment ameliorates CEES-induced cellular oxidative stress in mouse skin epidermal JB6 cells and human skin epidermal HaCaT cells

Mouse epidermal JB6 (A) and human epidermal HaCaT (B) cells were seeded and grown overnight in 96 well plates. These cells were then exposed to either DMSO alone (VC), 50 μM AEOL 10150 alone (AEOL), 0.25 mM CEES in DMSO (CEES), or to 50 μM AEOL 10150 1 h after 0.25 mM CEES exposure (CEES+AEOL) for 6 h. Thereafter, cells were incubated for 30 min with DHE (A and B), and the live cell fluorescence for the presence of ROS was determined using flowcytometry as described under Materials and Methods. Representative pictures of the flow cytograms of DHE stained JB6 and HaCaT cells with red

staining show increased ROS production, which was quantified (A and B). Data shown are mean ± SEM of 3 independent samples. *, $p<0.05$ as compared to CEES exposed group.

NIH-PA Author Manuscript
NIH-PA Author Manuscript
NIH-PA Author Manuscript

NIH-PA Author Manuscript
NIH-PA Author Manuscript
NIH-PA Author Manuscript

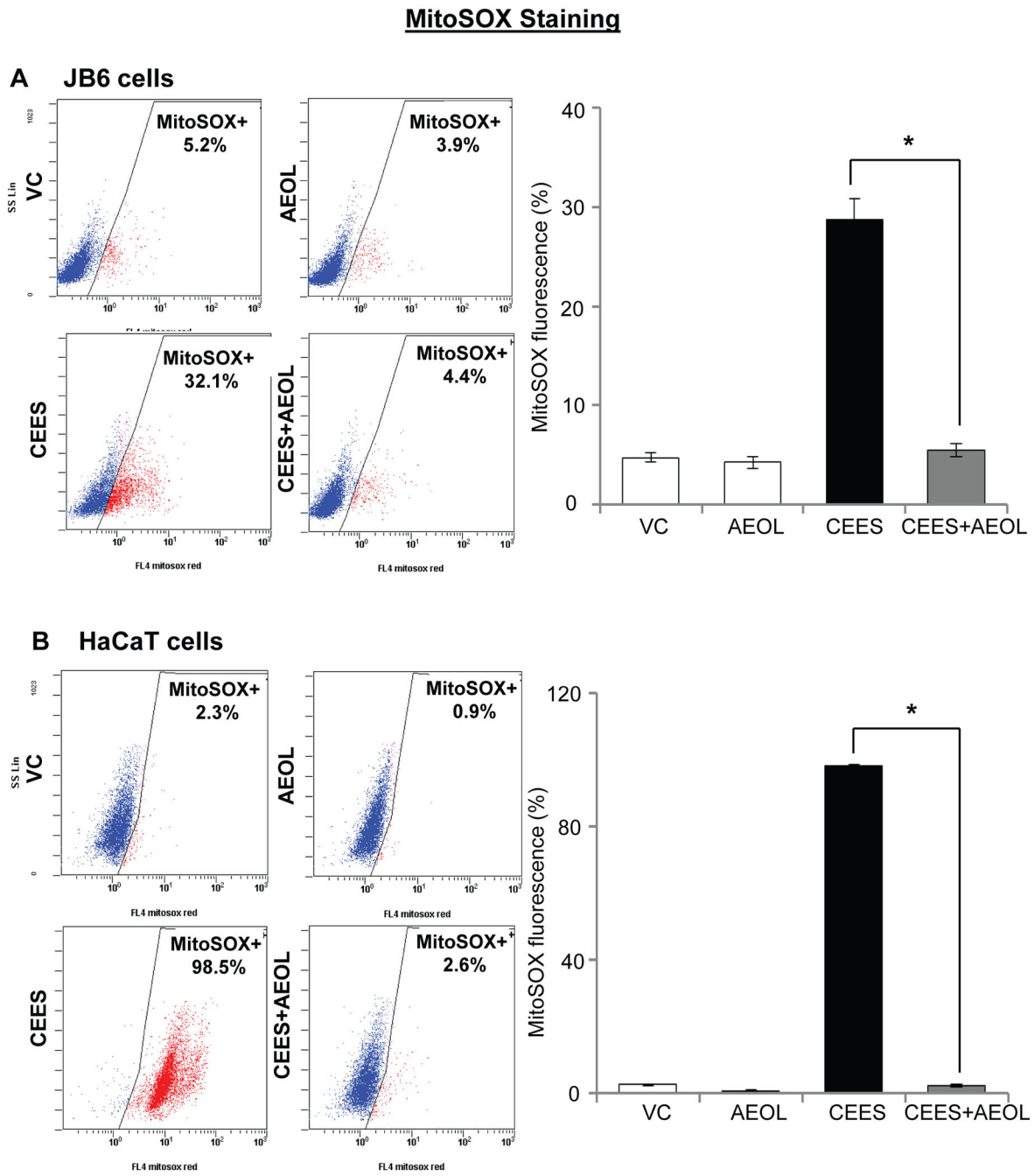

Figure 4. AEOL 10150 treatment ameliorates CEES-induced mitochondrial oxidative stress in mouse skin epidermal JB6 cells and human skin epidermal HaCaT cells

Mouse epidermal JB6 (A) and human epidermal HaCaT (B) cells were seeded and grown overnight in 96 well plates. These cells were then exposed to either DMSO alone (VC), 50 μM AEOL 10150 alone (AEOL), 0.25 mM CEES in DMSO (CEES), or to 50 μM AEOL 10150 1 h after 0.25 mM CEES exposure (CEES+AEOL) for 4 h. Thereafter, cells were incubated for 1 h MitoSOX Red (A and B), and the live cell fluorescence for presence of ROS was determined using flowcytometry as described under Materials and Methods. . Representative pictures of the flow cytograms of MitoSOX stained JB6 and HaCaT cells

NIH-PA Author Manuscript

NIH-PA Author Manuscript

NIH-PA Author Manuscript

with red staining show increased ROS production, which was quantified (A and B). Data shown are mean ± SEM of 3 independent samples. *, $p<0.05$ as compared to CEES exposed group.

NIH-PA Author Manuscript
NIH-PA Author Manuscript
NIH-PA Author Manuscript

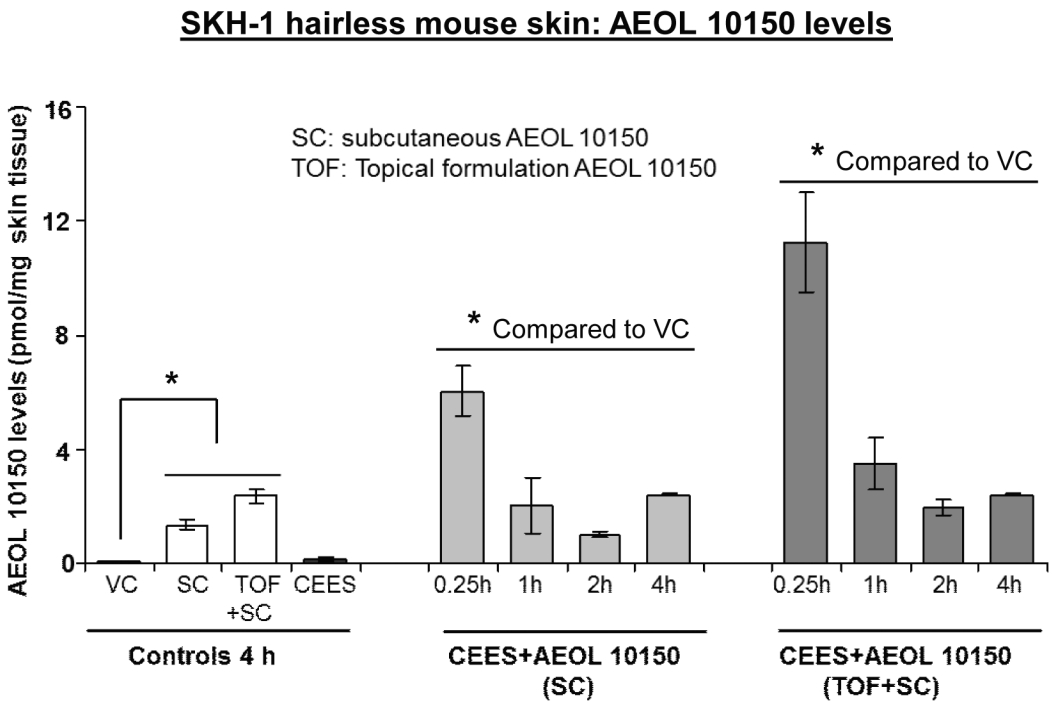

Figure 5. Effect of AEOL 10150 treatment on its levels in the SKH-1 hairless mouse skin tissue

Mouse dorsal skin was exposed topically to either 200 µl acetone (VC) or 4 mg CEES (CEES), or treated with subcutaneous AEOL 10150 (SC) or subcutaneous + topical AEOL 10150 (TOF+SC) 1 h after CEES exposure. After 15 min, 1, 2 and 4 h of exposure or treatments, skin samples were collected and pharmacokinetic study to measure AEOL 10150 levels in the skin was carried out using HPLC as detailed under Materials and Methods. Data shown are mean ± SEM of 3 independent samples from each group. *, $p<0.05$ as compared to vehicle control group.

NIH-PA Author Manuscript

NIH-PA Author Manuscript

NIH-PA Author Manuscript

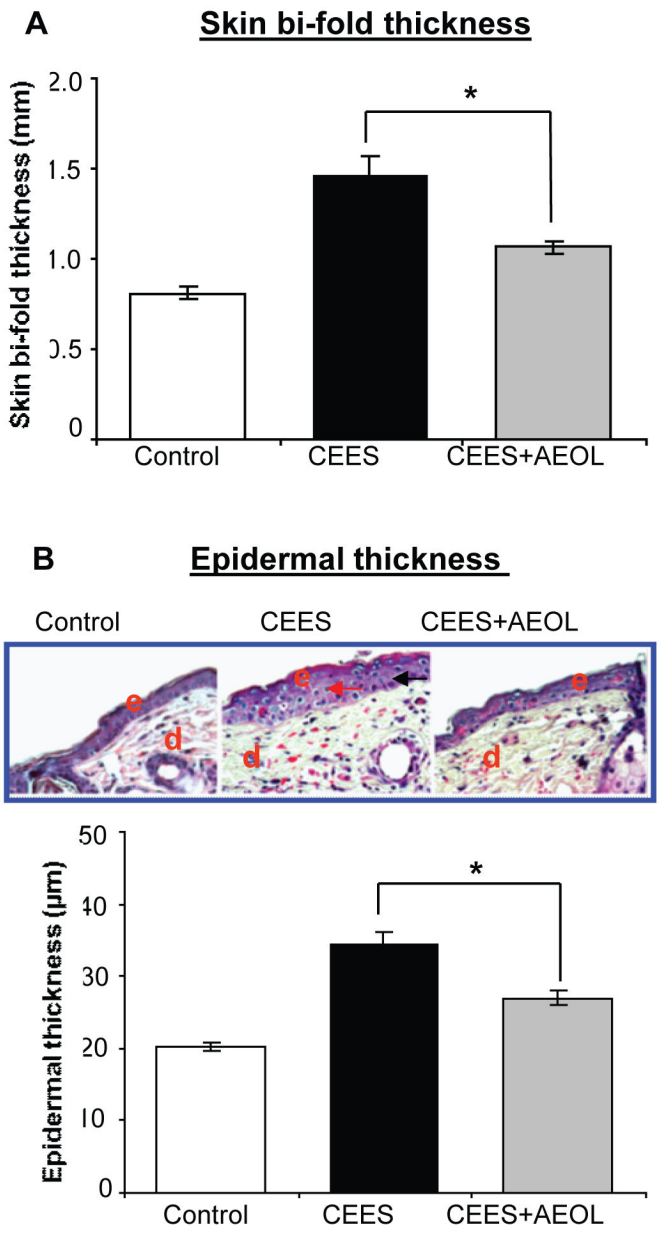

Figure 6. AEOL 10150 treatment ameliorates CEES-induced skin bi-fold thickness (A) and epidermal thickness (B) in SKH-1 hairless mouse

Mouse dorsal skin was exposed topically to either 200 μl acetone (VC) or 4 mg CEES (CEES), or treated with AEOL 10150 (subcutaneous + topical; CEES+AEOL) 1 h after CEES exposure as detailed under Materials and Methods. After 12 h of the indicated exposure or treatments, skin bi-fold thickness was measured using a digital caliper (A). Mice were sacrificed and dorsal skin tissue samples were collected at 12 h following the desired exposure or treatments, 5 μM skin sections were processed for H&E staining and analyzed for epidermal thickness (B). Representative H&E stained skin sections show epidermal thickness as well as quantified data for epidermal thickness (B). Data presented are mean ±

SEM (n=5); *, $p<0.05$ as compared to CEES exposed group. e, epidermis; d, dermis; red arrows, thickened epidermal layer.

NIH-PA Author Manuscript
NIH-PA Author Manuscript
NIH-PA Author Manuscript

NIH-PA Author Manuscript

NIH-PA Author Manuscript

NIH-PA Author Manuscript

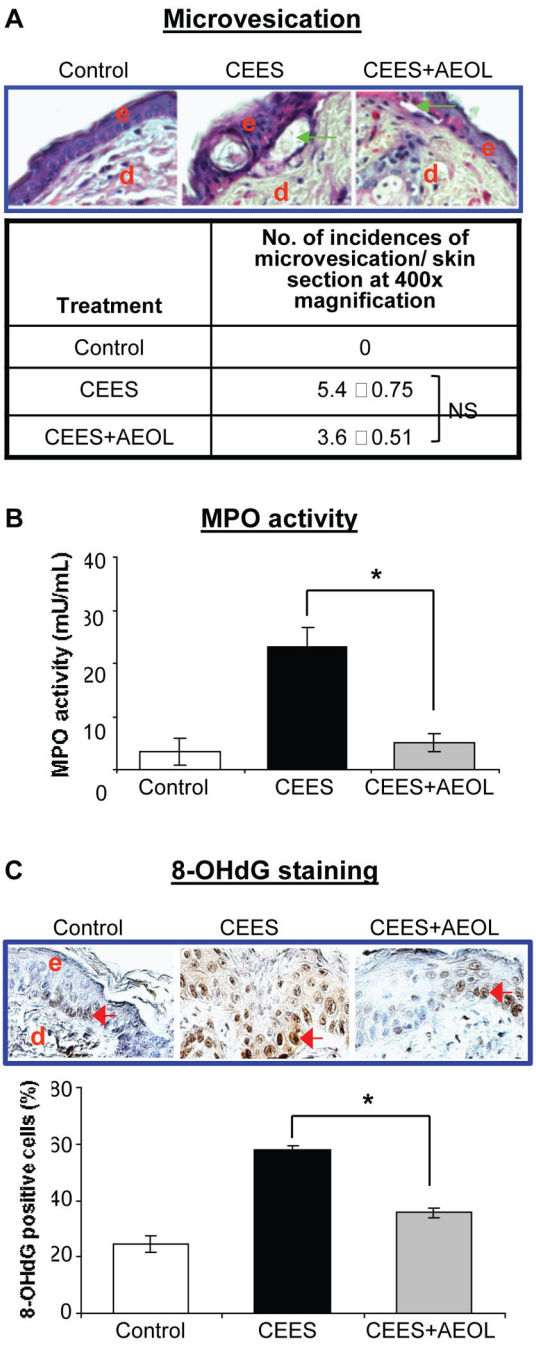

Figure 7. AEOL 10150 treatment effects on CEES-induced microvesication (A), myeloperoxidase activity (B) and DNA oxidation (C) in SKH-1 hairless mouse skin

Mouse dorsal skin was exposed topically to either 200 μl acetone (VC) or 4 mg CEES (CEES), or treated with AEOL 10150 (subcutaneous + topical; CEES+AEOL) 1 h after CEES exposure as detailed under Materials and Methods. After 12 h of the indicated exposure or treatments, mice were sacrificed and dorsal skin tissue samples were collected and either frozen or fixed as detailed under Materials and Methods. Skin tissue sections (5 μM) from fixed tissue were processed for H&E staining and analyzed for microvesication. (A) Representative H&E stained skin sections show microvesication as well as quantified

NIH-PA Author Manuscript

NIH-PA Author Manuscript

NIH-PA Author Manuscript

data for incidences of microvesiction (epidermal-dermal separation.. (B) Frozen skin tissue was used to determine MPO activity using a fluorescent kit from Cell Technology as detailed under Materials and Methods. (C) Skin sections (5 μm) from fixed tissue after processing were subjected to IHC for 8-OHdG as detailed under the Materials and Methods. The brown colored DAB positive nuclei were 8-OHdG positive (as shown in the representative pictures; C) and were counted in 10 randomly selected fields (400X magnification). Data presented are mean ± SEM (n=5); *, $p<0.05$ as compared to CEES exposed group; NS, not significant as compared to CEES group; e, epidermis; d, dermis; green arrows, epidermal-dermal separation; red arrows, 8-OHdG positive cells.

NIH-PA Author Manuscript

NIH-PA Author Manuscript

NIH-PA Author Manuscript

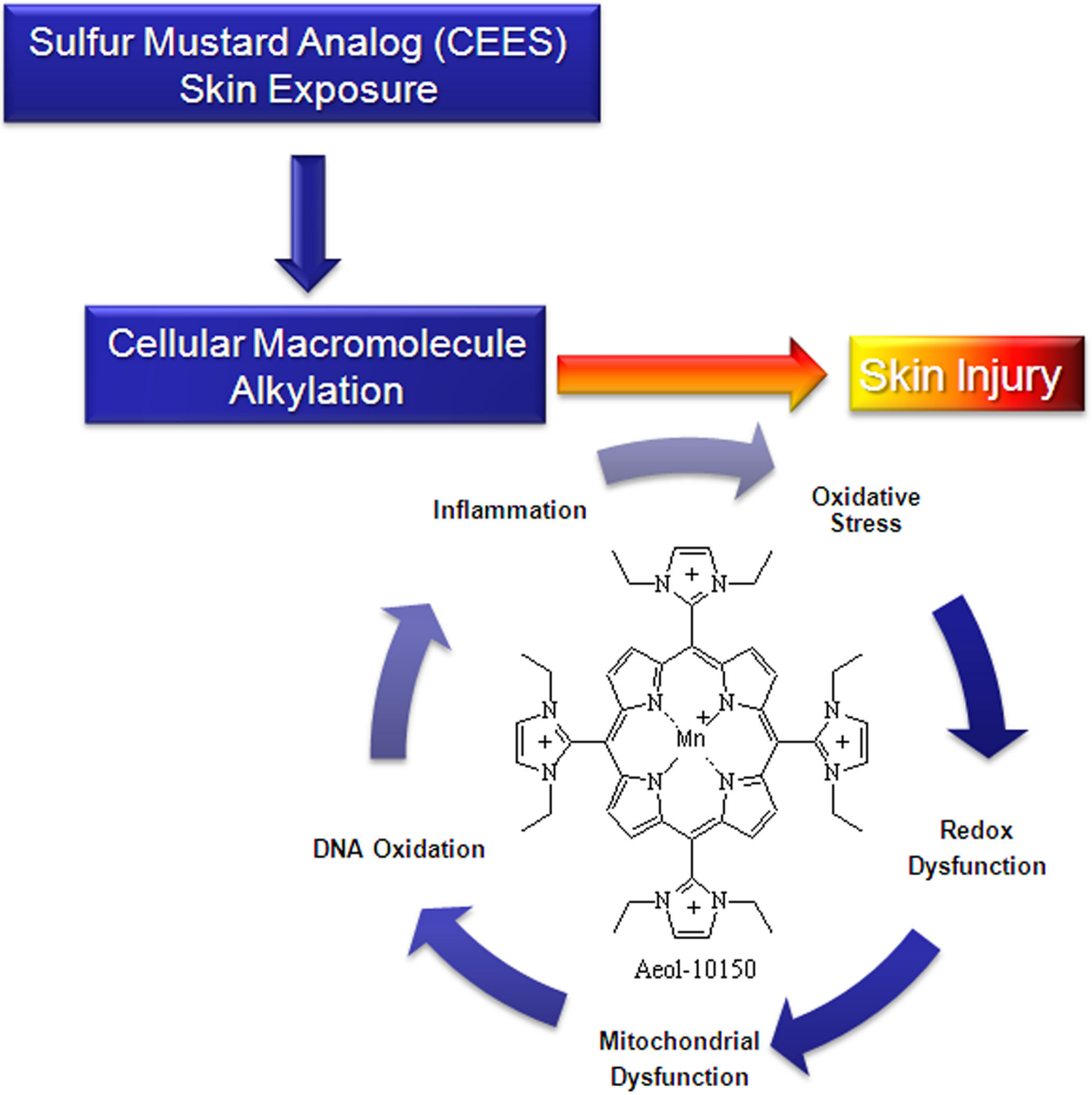

Fig. 8. Schematic of possible therapeutic targets for AEOL 10150 in CEES-induced skin injury pathways identified in our studies

The catalytic antioxidant AEOL 10150 attenuates downstream processes associated with sulfur mustard analog (CEES) macromolecule alkylation resulting in diminished oxidative stress, DNA damage, inflammation, and skin injury.